Magnetoresistance and spin frustration at low temperature in $LaMn_{1-x}Ni_xO_{3+\delta}$ ($0 \leq x \leq 0.1$)

2003 J. Phys.: Condens. Matter 15 4001

(http://iopscience.iop.org/0953-8984/15/23/312)

INSTITUTE OF PHYSICS PUBLISHING JOURNAL OF PHYSICS: CONDENSED MATTER

J. Phys.: Condens. Matter **15** (2003) 4001–4010 PII: S0953-8984(03)58695-7

Magnetoresistance and spin frustration at low temperature in $LaMn_{1-x}Ni_xO_{3+\delta}$ ($0 \leqslant x \leqslant 0.1$)

A Yamamoto and K Oda

Institute of Industrial Science, University of Tokyo, 4-6-1 Komaba, Meguro-Ku, Tokyo 153-8505, Japan

E-mail: akio@iis.u-tokyo.ac.jp

Received 23 January 2003, in final form 24 April 2003
Published 30 May 2003
Online at stacks.iop.org/JPhysCM/15/4001

Abstract

This paper investigates the relation between the temperature dependence of magnetoresistance (MR) and spin frustration in $LaMnO_{3+\delta}$ when Ni is doped into the Mn site. The specimens experience magnetic frustration introduced by the competition between antiferromagnetic (AFM) and ferromagnetic (FM) interactions. According to the temperature dependence of magnetization after cooling the specimen in zero field and non-zero field, Ni-doped specimens behave like cluster glasses. This magnetic frustration at the low temperature is believed to result from the disordered spin structure between AFM and FM phases in these specimens. When the structural symmetry in the specimen is higher, the FM arrangement increases by double the exchange interaction. However, MR decreases in the same temperature region for the same reason. We suggest that the temperature dependence of MR below the Curie temperature in the Ni-doped specimen is controlled by the change of magnetization that occurs with structural change.

1. Introduction

Perovskite manganites $La_{1-x}A_xMnO_3$ (A = Ca, Sr, etc) are known to show negative colossal magnetoresistance (CMR) effects [1–5]. The partial replacement of La^{3+} by A^{2+} ions causes the conversion of Mn^{3+} to Mn^{4+}, and the magnetic and transport properties of the manganites change. The mixed valency of Mn ions leads to strong ferromagnetic (FM) interaction arising from the Mn^{3+}–O–Mn^{4+} bonds. In general, it is considered that this FM interaction originates from the double exchange (DE) mechanism proposed by Zener [6]. According to the DE mechanism, charge carriers become itinerant among the FM interaction zones. The switching to the FM configuration is then facilitated by an applied field, and the percolative pathways between conductive parts are responsible for the observed large resistivity decrease. On the basis of this mechanism, the CMR effect in single crystalline manganites takes a maximum value at a temperature near the Curie temperature, T_C, due to

the metal–insulator transition (MIT). Furthermore, Hwang *et al* [7] have demonstrated that the large magnetoresistance (MR) in the polycrystalline $La_{2/3}Sr_{1/3}MnO_3$ exhibits two different behaviours; the large MR at low field dominated by spin-polarized tunnelling between grains and the high field MR which was remarkably temperature independent between 5 and 280 K.

It is well known that 3d magnetic metal ions form stable perovskite oxides together with rare earth ions which show various magnetic and transport behaviours. Furthermore, Mn^{3+} ions are Jahn–Teller ions, and the radius of Ni^{2+} ions is still larger than that of Mn^{3+} ions. Therefore, by substituting Mn^{3+} ions with Ni^{2+} ions, we expect further strain to be induced. Asai *et al* [8] proposed that nickel is in the divalent state, and that Ni^{2+} and Mn^{4+} align ferromagnetically, also based on the superexchange (SE) interaction between Ni^{2+}–O–Mn^{4+}. Hébert *et al* [9] also indicated from the investigation for $LaMn_{1-x}Ni_xO_3$ ($x \leqslant 0.2$) that nickel behaves like a divalent cation. The theory of the role of covalence in the perovskite-type manganites has been reported by Goodenough [10]. According to his theory, Mn^{3+} and Ni^{2+}, or Mn^{4+} and Ni^{2+}, align ferromagnetically. It would be interesting to study the charge mobility, MR and magnetization from the point of view of the magnetic exchange interaction within the Mn–O–Mn network when the partial replacement of Mn^{3+} by Ni^{2+} ions causes the conversion of Mn^{3+} to Mn^{4+}.

Wollan and Koehler [11] have reported that in $LaMnO_{3+\delta}$, the magnetic coupling between Mn^{3+} and Mn^{3+} or Mn^{4+} and Mn^{4+} is FM in the x–y plane and antiferromagnetic (AFM) along the z axis due to the SE interaction. They have also reported that in $LaMnO_{3+\delta}$ containing from 9 to 20% Mn^{4+}, there are regions or domains having AFM and FM ordering.

Fäth *et al* [12] investigated single crystals and thin films of $La_{1-x}Ca_xMnO_3$ by using scanning tunnelling spectroscopy. They showed that below T_C a phase separation (PS) is observed where inhomogeneous structures of metallic and more insulating areas coexist and are strongly field dependent in their size and structure. Uehara *et al* [13] showed that in $La_{5/8-y}Pr_yCa_{3/8}MnO_3$ at $y \sim 0.35$ giant clusters of FM and charge ordered (CO) phases coexist at low temperature. Furthermore, Moreo *et al* [14, 15] have reported the generation of large coexisting metallic and insulating clusters in doped manganites by computational studies. From these studies, it is natural to assume a ferromagnetically ordered region or cluster within the AFM matrix in $LaMn_{1-x}Ni_xO_{3+\delta}$.

So, in this paper we report the temperature dependence of magnetization after cooling the sample in zero magnetic field, zero field cooling (ZFC) and in field cooling (FC) in order to investigate the relation between the temperature dependence of MR and magnetic properties. We discuss the relationships connecting MR, magnetization and structural changes.

2. Experimental details

In order to investigate MR and magnetic properties of Ni-doped manganites, we prepared specimens with the compositions $LaMn_{1-x}Ni_xO_{3+\delta}$ ($x = 0, 0.01, 0.03, 0.1$) by the conventional solid state reaction method. La_2O_3, MnO_2 and NiO powders were mixed in the correct ratios for more than 2 h, pressed into pellets and calcined in air at 1223 K for 12 h. In the case of La_2O_3, in order to dehydrate the $La(OH)_3$ completely into La_2O_3, the powder was heated in vacuum and then sealed in a glass tube. The proper ratios of MnO_2 and NiO were derived from the precise composition of materials obtained by inductively coupled plasma (ICP) spectrometry. The pellets were ground for 2 h, pressed again and sintered in air at 1473 K for 18 h.

The phases of prepared specimens were identified by the x-ray powder diffraction method. The precise lattice parameter was measured by mixing the specimen with Si powder. The MR measurements were performed with and without applying external magnetic field with a

Table 1. The ratio of B sites occupied by Mn^{4+} ions. The magnetization observed at 30 K, together with the calculated one is also listed. The calculated value was obtained by the concentration of Mn^{4+} ions.

x	$Mn^{4+}/(Mn + Ni)$	M (experimental) (μ_B)	M (calculated) (μ_B)
0	0.11	2.96	4.0
0.01	0.25	3.36	3.7
0.03	0.15	3.69	3.8
0.10	0.18	3.41	3.7

temperature interval of 20 K between 300 K and a low temperature. The interval of the magnetic field was 0.5 T between +5 and −5 T. Resistivity was measured by the four-probe method and the current direction was parallel to the magnetic field. The amount of Mn^{4+} was determined by iodometric titrations using sodium thiosulfate. Temperature dependence of magnetization (MT) curves and magnetic field dependence (MH) curves at several temperatures were measured by a vibrating sample magnetometer (VSM) produced by Toei Industry. This VSM can apply a magnetic field of maxima 10 T with a He-free magnet. We measured MT curves after cooling the specimen from 290 to 30 K in zero field (ZFC) or in a field of 7 mT (70 Oe) (FC). And we also measured the temperature dependence of the linear ac susceptibility at several frequencies of magnetic field for $LaMn_{0.9}Ni_{0.1}O_{3+\delta}$.

3. Results and discussion

This paper is partly an extension of our previous work related to the electromagnetic properties of $LaMn_{1-x}Ni_xO_{3+\delta}$ ($0 \leqslant x \leqslant 0.1$) [16]. All produced specimens are confirmed to be perovskite single-phase type. The symmetry is hexagonal. For the x-ray diffraction patterns, see the preceding paper. In table 1, the ratio of Mn^{4+} ions for each specimen measured by ICP and iodometric titrations is shown. We have reported earlier that all specimens contained excess oxygen. The amount of excess oxygen, δ, ranges from 0.15 to 0.18 in the specimens. The amount of $Mn^{4+}/(Mn + Ni)$ increase from 0.15 to 0.18 when the amount of Ni substitution increases from 3 to 10%. We propose that Ni ions exist as Ni^{2+}. This is consistent with the result of Hébert *et al* [9]. The reason why the 1% Ni-doped specimen has the highest amount of Mn^{4+} is presumed to be because it contains a larger amount of excess oxygen than the other specimens. For details regarding the amount of Mn^{4+}, see the preceding paper [16]. Here, our discussions assume that all of the Ni ions in $LaMn_{1-x}Ni_xO_{3+\delta}$ ($0 \leqslant x \leqslant 0.1$) are Ni^{2+}.

Figure 1 shows the temperature dependence of resistivity (upper graph) and MR effect (lower graph) in $LaMn_{0.9}Ni_{0.1}O_{3+\delta}$. (The magnitude of MR $= (\rho_{0T} - \rho_{5T})/\rho_{0T}$, where ρ_{0T} and ρ_{5T} are the resistivities without a magnetic field and with a field of 5 T, respectively.) We have pointed out that the specimens in which the Mn sites are doped with Ni do not exhibit MIT, while the $LaMnO_{3+\delta}$ specimen did. The reason for this difference was explained by the existence of the excess oxygen and the deviation of the Mn/La ratio from unity [16, 18]. It is important that $LaMn_{1-x}Ni_xO_{3+\delta}$ had the same mixed valency of Mn as in $La_{1-x}A_xMnO_3$ (A = Ca, Sr), nevertheless, no MIT was observed. From these results, it has been derived that Mn^{3+} ions adjacent to Ni^{2+} do not change to Mn^{4+} and the mobility of carriers is suppressed due to the SE interactions between Ni^{2+} and Mn ions. Consequently, the percolative pathways between conductive parts decrease in comparison with $La_{1-x}A_xMnO_3$ which shows a MIT. This has been proposed as the reason why the maximum of the CMR decreases as the ratio of $Ni/(Mn + Ni)$ increases [16]. Moreover, when decreasing the temperature below T_C, first a decrease and then an increase of the MR has been observed in

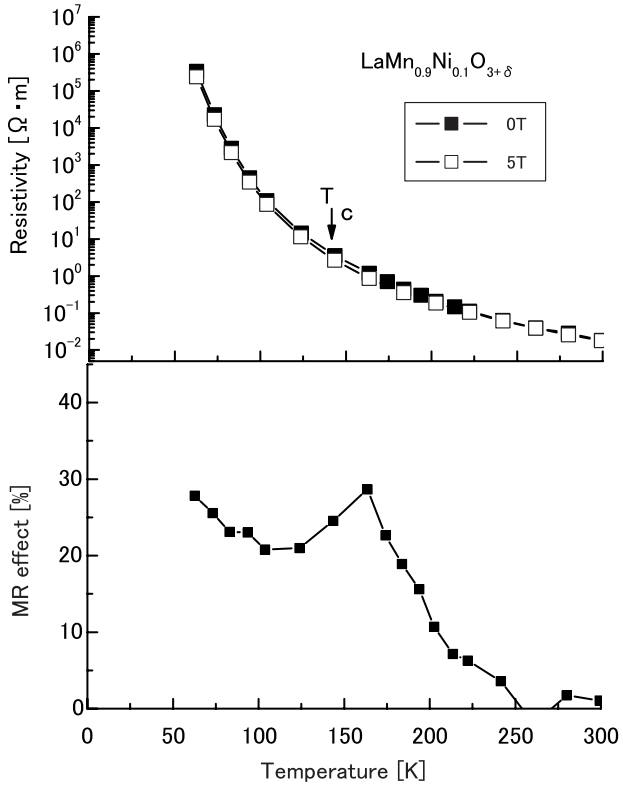

Figure 1. The temperature dependence of resistivity and the MR effect.

the Ni-doped specimens. This temperature dependence of the MR differs from that observed in $La_{2/3}Sr_{1/3}MnO_3$ or $La_{0.67}Sr_{0.33}Mn_{0.80}Ni_{0.20}O_3$ and the effect keeps on increasing when decreasing the temperature [7, 17]. It is impossible to explain this increase/decrease at the temperature below T_C only by the DE interaction and/or the grain boundary effect in the polycrystalline specimens. The magnetic frustration could be responsible for this peculiar temperature dependence that has been observed in our previous results. As a next step, we can expect that the coexistence of FM and AFM regions can produce a magnetic frustration in the lower temperature region.

3.1. The magnetic field dependence of magnetization

Figure 2 shows the MH curves measured at 30 K. It can be seen that all of the specimens indicate ferromagnetism at this temperature. The reason why $LaMnO_{3+\delta}$ is FM is presumed to be the high amount of Mn^{4+} due to excess oxygen. The spontaneous magnetizations, derived experimentally by extrapolating magnetization to zero field in the MH plot based on the high field data, are also shown in table 1. Assuming that Mn^{4+}, Mn^{3+} and Ni^{2+} take a FM alignment, the magnetization of each specimen, which is calculated from the Mn^{4+}, Mn^{3+} and Ni^{2+} concentrations obtained by ICP measurement and iodometric titrations, can be calculated. Here, the effective Bohr magneton of Mn^{3+}, Mn^{4+} and Ni^{2+} ions are 4, 3 and 2, respectively. The calculated results are also summarized in table 1. When increasing the doping amount of Ni, the change of the spontaneous magnetization corresponds well to that of the calculated one.

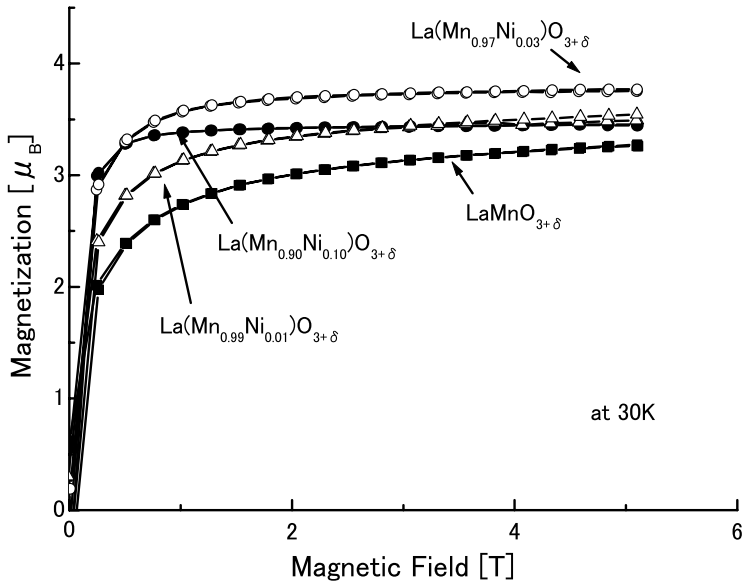

Figure 2. Magnetic field dependence of magnetization.

This indicates that the magnetic interactions between Ni^{2+} and Mn^{4+} or Ni^{2+} and Mn^{3+} are FM in the specimen. Moreover, M (experimental) is smaller than M (calculated) in all of the specimens. It can be expected from these results that the specimens have magnetically frustrated areas introduced by the competition between AFM and FM interactions. We have observed that the temperature dependence of the magnetization at high field increases below T_C as the temperature decreases. So, at high field the FM phase increases below T_C as the temperature decreases. From these results, it can be imagined that the MR of $LaMn_{0.9}Ni_{0.1}O_{3+\delta}$ in a magnetic field of 5 T is high enough to orient magnetic domains but not enough to affect the AFM phase. As a next step, we show the temperature dependence of magnetization at low field.

3.2. The temperature dependence of magnetization

Figure 3 shows the MT curves for the FC and ZFC cases. The ZFC process is as follows; after the specimen was zero field cooled down from room temperature to 30 K, a magnetic field of 5 T was applied once for a few seconds. Then, the magnitude of the field was switched to 70 Oe at the same temperature. Hence, the temperature dependence of the M_{ZFC} was measured in a warming process with a field of 70 Oe applied. All specimens exhibit spontaneous magnetization below T_C. Furthermore, it can be seen that in Ni-doped specimens, the temperature dependence of the M_{FC} gradually coincides with that of the M_{ZFC} with increasing temperature, while a large deviation between the two curves exists at the low temperature. It will be helpful to classify the temperature dependence of M_{ZFC} into three regions. They are the temperature regions (i) below T_s, (ii) between T_s and T_f and (iii) above T_f. Here, T_s is the minimum temperature of the temperature region where M_{ZFC} shows a peak with a moderate slope. T_f is the temperature where M_{ZFC} is a maximum. The difference between M_{ZFC} and M_{FC} could be due to the magnetic frustration introduced by AFM and FM interactions [19, 20]. However, the difference between the temperature dependence of M_{ZFC}

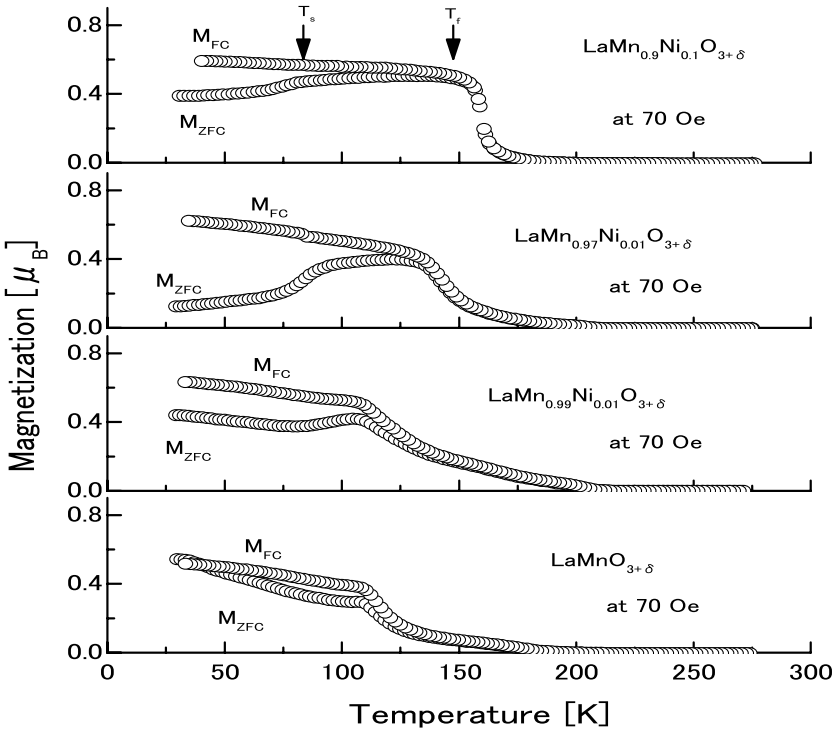

Figure 3. The temperature dependence of the magnetization, $M(T)$, after cooling the sample from 290 to 30 K in zero field (ZFC) or in a field of 70 Oe (FC).

below T_s and between T_s and T_f cannot be explained by a normal spin glass frustration for AFM and FM interactions. This irreversibility between M_{ZFC} and M_{FC} indicates the existence of a cluster glass. The cluster glass is characterized by the large deviation between M_{ZFC} and M_{FC} at low temperatures and a gradual reduction of M_{ZFC} with decreasing temperature and so on [19, 20]. We suggest that the competition between the clusters of the FM regions and those of the AFM regions introduces magnetic frustration. So, we propose that at low field FM regions are small and cluster-like below T_s and they grow between T_s and T_f at low field. However, recall the temperature dependence of the magnetization that increases at high field below T_C as the temperature is decreased. According to this result, at high field, the FM phase is actually increasing below T_C as the temperature decreases. These results at low and high field indicate that the extent of the FM regions below T_s grows with applied field.

In the case of $LaMn_{0.99}Ni_{0.01}O_{3+\delta}$, both M_{ZFC} and M_{FC} decrease when the temperature is increased below T_s. This suggests that the frustration is small in this case below T_s. This is probably because the ratio of Mn^{4+} is large (table 1) and also because the amount of Ni^{2+} is less. Consequently, the rate of FM coupling between Mn^{3+} and Mn^{4+} in this specimen is larger than in the other Ni-doped specimens, and the spin frustration due to the chemical substitution is small.

By increasing the ratio of Ni/(Mn + Ni) from 3 to 10%, the difference between M_{ZFC} and M_{FC} below T_s becomes small. The temperature region of M_{ZFC} between T_s and T_f also broadens as the Ni concentration is increased. We propose from these results that by increasing the amount of Ni the FM cluster grows larger at lower temperatures.

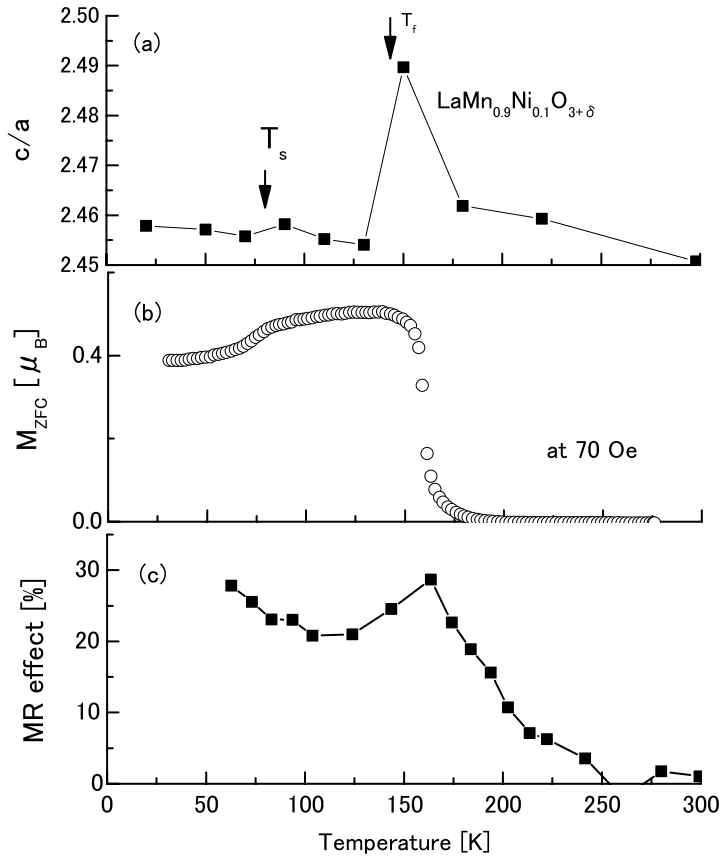

Figure 4. The temperature dependence of (a) c/a, (b) M_{ZFC} and (c) the MR effect in $LaMn_{0.9}Ni_{0.1}O_{3+\delta}$.

3.3. The relationships connecting the MR effect, the magnetization and structural symmetry

Figure 4(a) shows the temperature dependence of ratio of the lattice parameter, c/a, at zero field in $LaMn_{0.9}Ni_{0.1}O_{3+\delta}$. Here, the hexagonal basis is applied. When c/a is equal to 2.45, the structural symmetry is cubic. As c/a deviates from 2.45, distortion is introduced. Figure 4(b) shows the temperature dependence of M_{ZFC} at 70 Oe in $LaMn_{0.9}Ni_{0.1}O_{3+\delta}$ for comparison. It can be seen from figure 4(a) that there exist peaks of c/a at around T_f and T_s. It can also be seen that c/a is slightly larger below T_s than between T_s and T_f. These results indicate that the FM phase is stable by the DE interaction when c/a is close to 2.45. They also indicate that FM regions at zero field are smaller below T_s than between T_s and T_f. From these indications we propose that the ratio of the FM phase to the AFM phase is decided by structural change. Figure 4(c) shows the temperature dependence of the MR effect in $LaMn_{0.9}Ni_{0.1}O_{3+\delta}$ (the same as in figure 1 (lower graph)). At $T < T_s$ as c/a increases from 2.45, MR also increases. Also, the MR effect is larger below T_s than it is between T_s and T_f. These results show that charge carriers are moved more smoothly by the DE interaction when c/a is closer to 2.45. It is interesting that the MR effect is related to the difference between the extent of the FM region whether or not a constant field is applied, for the specimen having no MIT. These phenomena suggest that not only the DE interaction but also the differences in the carriers' mobilities, originating from structural symmetry, are necessary to explain the origin of MR

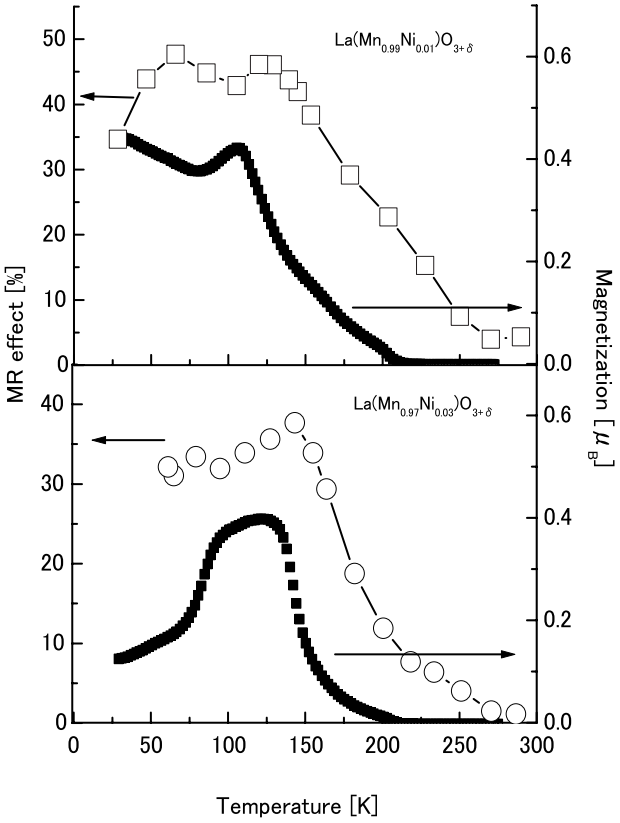

Figure 5. The temperature dependence of the MR effect (open symbols) and ZFC magnetization (solid symbols) at 70 Oe.

in this series of oxides. Since the amount of Mn^{4+} and the substitution of Ni maintain the insulation by giving a good balancing ratio of the FM and AFM regions in our specimens, we propose that an increase/decrease of the temperature dependence of the MR effect occurs. Figure 5 shows the temperature dependence of M_{ZFC} and the MR effect in $LaMn_{0.99}Ni_{0.01}O_{3+\delta}$ and $LaMn_{0.97}Ni_{0.03}O_{3+\delta}$. It is also found that M_{ZFC} and the MR effect are related.

3.4. The temperature dependence of ac susceptibility

Figure 6 shows the temperature dependence of the ac susceptibility of $LaMn_{0.9}Ni_{0.1}O_{3+\delta}$ when an ac field of 0.1 mT (1 Oe) is applied in the frequency range between 20 and 500 Hz. There exists a frequency dependence of the temperature maxima of χ_1' and χ_1''. The peaks shift to higher temperature as the frequency increases. We have analysed this frequency dependence of the peak temperature by curve fitting the data following the Vogel–Fulcher law, $f = f_0 \exp(E_a/k(T_B - T_0))$. The result of the fitting is shown in figure 7. Here, $E_a/k_B = 382$, $f_0 = 107$ Hz and $T_0 = 118$ K are derived as fitting parameters in the frequency range between 20 and 500 Hz. From these parameters, $(T_f - T_0)/T_f = 0.25$ is obtained. This value is comparable to that of $La_{0.5}Sr_{0.5}CoO_3$ (=0.27), which is known to be a cluster glass [20]. This should also be proof for the existence of a cluster glass in $LaMn_{0.9}Ni_{0.1}O_{3+\delta}$.

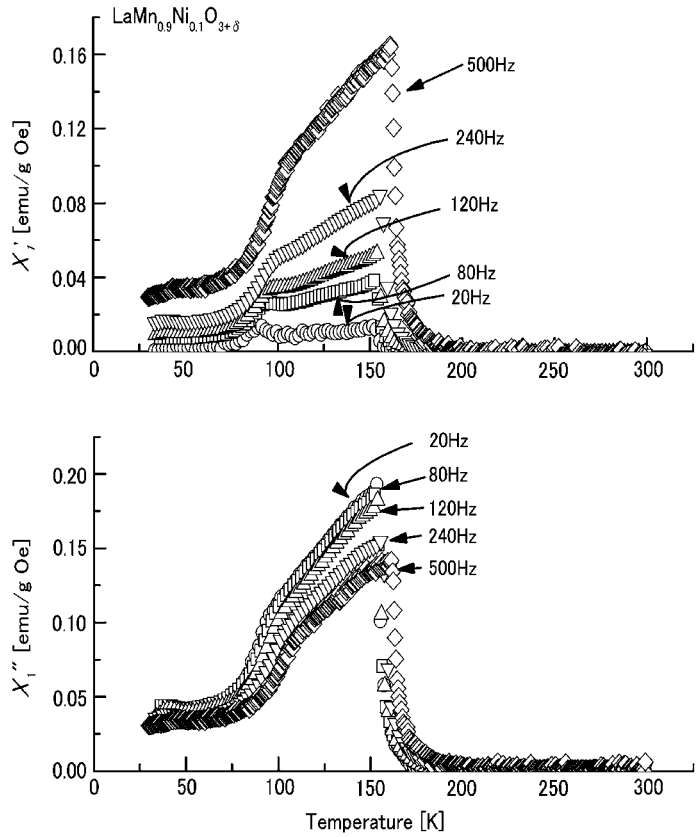

Figure 6. The linear ac susceptibility data measured at different frequencies for an ac field of 1 Oe in $LaMn_{0.9}Ni_{0.1}O_{3+\delta}$.

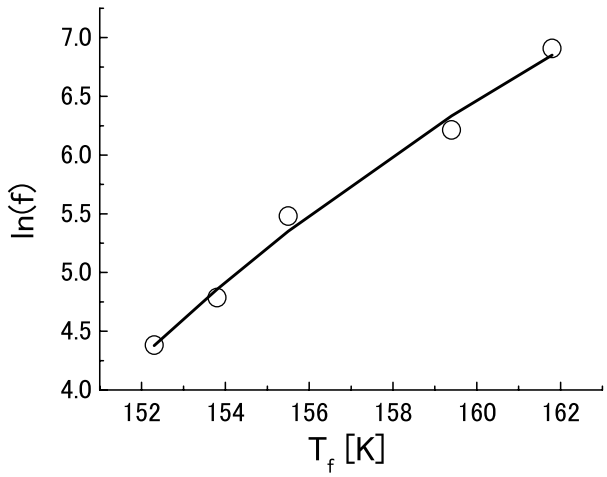

Figure 7. Curve fitting of the experimental data for χ_1'' from figure 6 using the Vogel–Fulcher law.

4. Conclusion

In summary, we measured the temperature dependence of M_{ZFC}, the MR effect and c/a, in particular for $LaMn_{0.9}Ni_{0.1}O_{3+\delta}$. The results of the temperature dependence of M_{ZFC} are related to c/a and the increase/decrease of the MR observed below T_C. We suggest that the temperature dependence of the MR effect in $LaMn_{1-x}Ni_xO_{3+\delta}$ ($0 \leqslant x \leqslant 0.1$) is related to the spin frustration with charge localization at lower temperature that is caused by the Ni^{2+} doped into Mn sites. We also suggest from these results that the control of the temperature dependence of the MR effect by replacement of only the B sites is possible.

Acknowledgments

This work is supported by the Grant-in-Aid for Specially Promoted Research from the Ministry of Education, Culture, Sports, Science and Technology (12CE2004 Control of Electrons by Quantum Dot Structures and Its Application to Advanced Electronics). Furthermore, the present research is supported in part by a Grant for the 21st Century COE Programme of Human-Friendly Materials Based on Chemistry from the Ministry of Education, Culture, Sports, Science and Technology of Japan.

References

[1] Jonker G H and van Santen J H 1950 *Physica* **16** 337
[2] Jonker G H and van Santen J H 1953 *Physica* **19** 120
[3] Chahara K *et al* 1993 *Appl. Phys. Lett.* **63** 1990
[4] Hundley M F and Neumeier J J 1997 *Phys. Rev.* B **55** 11511
[5] Laiho R *et al* 2000 *J. Phys.: Condens. Matter* **12** 5751
[6] Zener C 1951 *Phys. Rev.* **82** 403
[7] Hwang H Y *et al* 1996 *Phys. Rev. Lett.* **77** 2041
[8] Asai K *et al* 1998 *J. Phys. Soc. Japan* **67** 4218
[9] Hébert S *et al* 2002 *Phys. Rev.* B **65** 104420
[10] Goodenough J B 1955 *Phys. Rev.* **100** 564
[11] Wollan E O and Koehler W C 1955 *Phys. Rev.* **100** 545
[12] Fäth M *et al* 1999 *Science* **285** 1540
[13] Uehara M *et al* 1999 *Nature* **399** 560
[14] Moreo A *et al* 1999 *Science* **283** 2034
[15] Moreo A *et al* 2000 *Phys. Rev. Lett.* **24** 5568
[16] Yamamoto A and Oda K 2002 *J. Phys.: Condens. Matter* **14** 1075
[17] Wang Z H *et al* 1999 *J. Appl. Phys.* **85** 5399
[18] Töpfer J and Goodenough J B 1997 *Solid State Ion.* **101–103** 1215
[19] Itoh M *et al* 1994 *J. Phys. Soc. Japan* **63** 1486
[20] Mukherjee S and Ranganathan R 1996 *Phys. Rev.* B **54** 9267